Journal of Manufacturing Engineering, 2007, Vol.2, Issue.2

SIMULATION OF RATCHETING BEHAVIOR BY EXPERIMENTAL AND FINITE ELEMENT

Ajit G Dongarkar[1*] and Prof. Dr. P. Vasudevan[2]

[1]EACOE, John F Welch Technology Centre, Bangalore, India.
[2] Mechanical Engineering Department, IIT Bombay, Mumbai, India.

***E-mail:** ajit.Dongarkar@geind.ge.com

ABSTRACT

Ratcheting is a phenomenon in cyclic plasticity. It is defined as the accumulation of plastic strain with progressive load cycles. It is well known that ratcheting can reduce the fatigue life of the components subjected to cyclic load environment such as pressure vessel systems. For design and analysis of these types of structures, accurate prediction of ratcheting response is critical as ratcheting can lead to catastrophic failure of structures. Experimentation is carried out on SS304 tube specimens under uniaxial and biaxial set of loadings. The specimens are subjected to constant internal pressure and axially cyclic loading is applied using Universal Testing Machine. The strain data in axial and hoop directions is measured using strain gauges. The material parameters of the nonlinear Chaboche Model are determined with the data obtained from the experimentation. These material parameters are used in the commercial finite element program "ANSYS" to simulate the ratcheting behavior for different load histories and geometries. Comparison is made between experimental and FEM results to analyze the robustness of the Chaboche Model used in the simulation studies.

Keywords: *Fatigue, Ratcheting, Cyclic plasticity, Von Mises Criteria, SS304, Stress-Strain Curve, Hysteresis Loop, ANSYS, Hardening, Stabilization,*

1. INTRODUCTION

Engineering components and structures are often subjected to cyclically varying loads with mean stress. The ratcheting phenomenon corresponds to a regular progression of plastic strain, cycle by cycle which leads to an excessive deformation. Even for structures that are designed to be within the elastic limit, plastic zones may exist at discontinuities or at the tip of cracks. The fatigue cracks can initiate at these plastic zones. Therefore, better simulation model for cyclic plasticity response is important for the prediction of the high cycle fatigue life as well.

Many components or structures undergoing mechanical or thermal cyclic (secondary type) loads while subjected to sustained (primary type) loadings are liable to undergo strain accumulations which can affect their mode of failure. If the mode of failure is ratcheting or fatigue with ratcheting, then the allowable stresses based on plastic collapse load can be overly conservative. The phenomenon falls into the broader subject of cyclic plasticity which has received considerable attention over the last twenty years. This has included micromechanical as well as macro mechanical investigations which have led to development of significant number of models of elastic-plastic material behavior under complex, cyclic loadings. The modeling of cyclic plasticity responses is quite complex. Experimental studies demonstrate that the yield surface grows (isotropic hardening), translates (kinematic hardening) as well as changes shape (formative hardening) with plastic loading. Some metals harden, while many others soften during plastic cyclic loading. Moreover, the cyclic plasticity responses are history dependent.

Although most metals cyclically harden or soften up to certain number of cycles, they subsequently stabilize. Ratcheting strains, however, keep on accumulating with cycles even after the material stabilizes. This is called as pure ratcheting by some authors and the kinematical hardening is attributed to be the primary reason for pure ratcheting. Motivated by the need for an analysis tool which can accurately simulate ratcheting in piping components (e.g. straight pipes, elbows and branch pipes), an attempt is made here to carry out ratcheting simulations in ANSYS, a widely used finite element program. The material parameters for the cyclic plasticity models are obtained by carrying out experimentation on one inch SS 304 tube specimens. These tube specimens are tested using 50kN universal testing machine and the strain data is acquired from axial and hoop directions using post-yield rectangular strain gauge rosette. The simulations carried out using ANSYS for uniaxial and biaxial are compared with the results obtained from experimental work.

2. EXPERIMENTAL DETAILS

The main aim of experimentation done in this project was to find out the material model parameters for Chaboche's Nonlinear Kinematic Hardening Model and then to compare the results of FEM with the actual experiments for same load histories and geometry of the specimen. The Figure 1 below shows the Hysteresis loop for the material in plastic loading range. The basic information on the cyclic stress strain behavior of a material is provided in the form of the stress-strain hysteresis loop. Some of the important quantities that are used for the Chaboche Model are given in the figure.

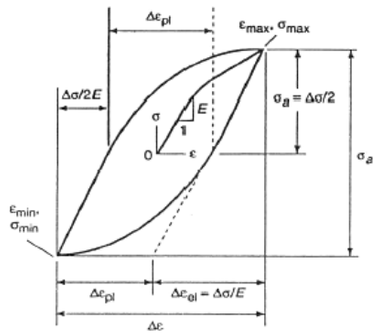

Figure 1 - Primary Quantities of the Hysteresis Loop

The material used for this test is SS 304 seamless tube of 23.4 mm diameter in gauge section and 2 mm thickness in gauge section. This material is obtained from Reactor Safety Division (RSD), Bhabha Atomic Research Center (BARC) Mumbai for the experimentation purpose. This is austenitic stainless steel and is cyclic hardening material. The specimens were prepared at IIT Bombay and the detailed drawing of the specimen is given in figure 2 below. The photograph of the strain-gauged specimen is shown in Figure 3.

Figure 3 - Tube Specimen for Ratcheting Testing.

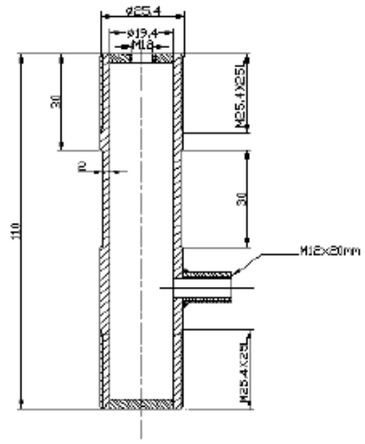

Figure 2- Tube Specimen for Ratcheting Testing.

The tests are carried out on 50 KN capacity universal testing machine. The tube specimens are pressurized with water for the biaxial test using a reciprocating type hand pump. The specimen has two openings: one inlet to the pump and other end is closed after removal of air completely from the system. This ensures that bursting due to air trapped inside will be avoided in case of failure of the specimen. The internal pressure in maintained constant throughout the test. The pressure was increased upto 200 bar and adequate waterproof covering was provided around the sample to avoid the possibility of water spilling over the machine in case of leakage through the specimen.

3. STABILISED HYSTERESIS LOOP

All the three samples tested were first stabilized using strain controlled axial cycling. This will essentially remove the effect of isotropic hardening from further experimentation which will be used for ratcheting. The stabilized hysteresis loop of axial stress Vs axial strain is shown in figure 4. This will be used for finding out the parameters of the kinematic hardening model

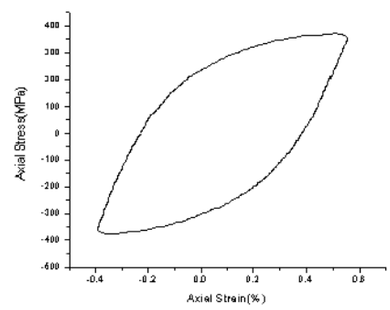

Figure 4 - Stabilized Hysteresis Loop for SS 304

The SS 304 material shows the strain hardening characteristics and gets stabilized after few cycles only. The modulus of elasticity of this material was found to be 2.01 x 10^5 Mpa and the initial yield stress was 239 Mpa.

4. RATCHETING EXPERIMENTS

The loading histories of the experiment set are shown in Figure 5. The history in Figure 5 a) which results in ratcheting of axial strains, involves axial stress controlled cycles with a mean stress. The loading history in Figure 5 b) involves axial strain cycles in presence of a constant internal pressure. The history results in ratcheting of the circumferential strain.

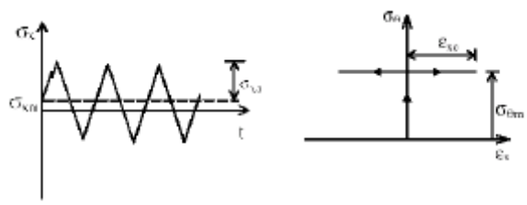

(a) (b)

Figure 5 - Loading Histories a) Uniaxial Stress Cycles, b) Symmetric Axial Strain Cycling with Constant Pressure

5. UNIAXIAL RATCHETING TESTS

Uniaxial ratcheting tests are essential for finding out the material parameters of the Chaboche's model. Here two specimens were tested for uniaxial stress controlled cyclic loading with a mean stress. The presence of mean stress is essential for the accumulation of the strain in the mean stress direction in case of uniaxial ratcheting. One specimen was tested with positive stress ratio and other with negative stress ratio. The data is acquired from both axial and circumferential directions during the test. The tests were conducted till the axial strain reaches the strain gauge capacity of 3%.

5.1 Test with Mean Stress of 278 Mpa and Stress Ratio 0.54

This stress controlled uniaxial tests was continued till full capacity of the axial strain gauge (3%) is utilized. The Figure 6 shows the plot of axial stress Vs axial strain and Figure. 7 shows the plot of axial stress Vs hoop Strain. The ratcheting accumulation was found to be higher in the first few cycles and later, the rate of ratcheting was found to be decreased and remain constant. There was no shakedown observed till the end of the test. Same pattern of strain accumulation in negative direction is observed in circumferential direction.

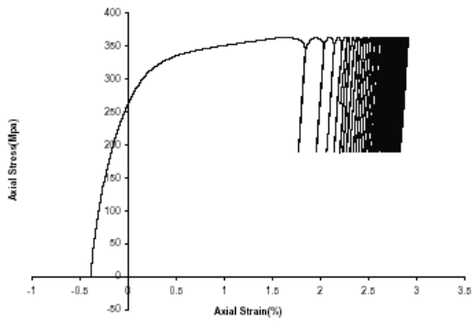

Figure 6 - Plot of Axial Stress vs. Axial Strain for First Uniaxial Ratcheting Test

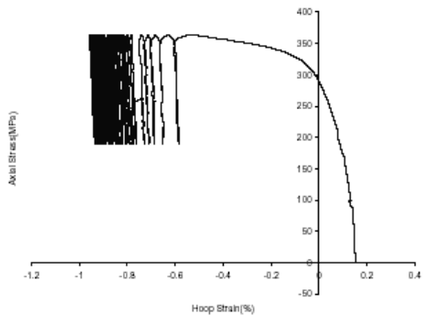

Figure 7 - Plot of Axial Stress vs. Hoop Strain for First Uniaxial Ratcheting Test

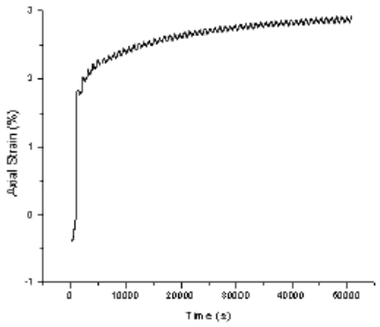

Figure 8 - Plot of Axial Strain vs. Test Duration for First Uniaxial Test

The variation of axial strain with respect to time is given in Figure 8. Here it is clearly seen that the ratcheting rate decreases and attains a constant value after initial few cycles.

5.2 Test with Mean Stress of 75 Mpa and Stress Ratio 0.6

In this test, negative stress ratio was chosen and testing was continued upto 3.5% strain accumulation in axial direction. The ratcheting rate was initially high, later became almost constant and remained constant throughout the test. This behavior is same as obtained during the positive stress ratio test. Figure. 9 shows the plot of axial stress vs. axial strain and Figure 10 shows the plot of axial strain against the duration of the test. The test was stopped after about 93 hours as there was no sign of shakedown and also sufficient data was acquired for tuning of the Chaboche's material model. Out of these two uniaxial tests discussed so far, the later case is simulated in ANSYS and the tuning of the Chaboche model (value of γ_3) is done. The former test is used for comparison of the test results with the one obtained using finite element method.

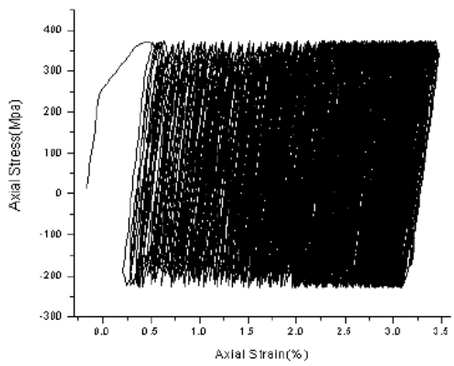

Figure 9 - Plot of Axial Stress vs. Axial Strain for Second Uniaxial Test

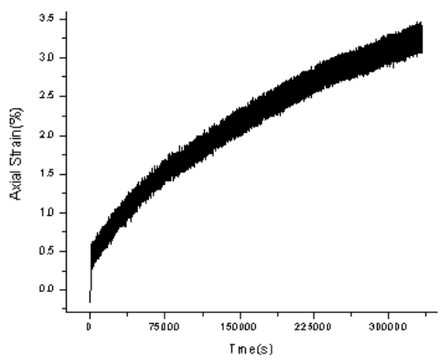

Figure 10 - Plot of Axial Strain vs. Duration of the Test for Second Uniaxial Test

6. BIAXIAL RATCHETING TEST

The biaxial ratcheting test is done with pressurizing the tube specimen such that the hoop stress developed is below the uniaxial yield stress of the specimen and then axial strain cycling within limit of ±0.5%. Note that the strain corresponding to the initial yield point of 239 Mpa is 0.12%. So here the secondary strain cycling is done in plastic range while the stress due to primary load (internal pressure) is within the elastic limit of the specimen. The test is started with 100 bar internal pressure (hoop stress 52.5Mpa). The ratcheting of the hoop strain was observed for the first 20 cycles and is followed by shakedown at the value of hoop strain equal to 0.33%. The internal pressure was then increased to 150 bar hoop stress 78.75Mpa) and the test was continued for 250 cycles. The ratcheting rate was almost constant and there was no indication of any shakedown. The ratcheting was proceeding at very slow rate and the hoop strain accumulated up to 1.45%. Since the test was taking enormous time, it was decided to increase the internal pressure further to 200 bar (hoop stress 105Mpa) in order to accelerate the test. The post test observation of the specimen shape by naked eye clearly shows that it has bulged out due to hoop strain ratcheting. Figure 11 shows the plot of hoop strain vs. test duration and the total test duration for this test was about 143 hours.

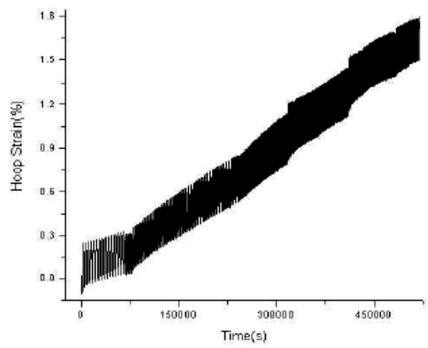

Figure 11-Plot of Hoop Strain vs. Test Duration for Biaxial Test

The plot of axial load vs. hoop strain accumulation is given in Figure .12. It becomes clear that for total 389 cycles done, the ratcheting rate was very small and the material shows promise in showing the biaxial ratcheting behavior. This loading history of 389 cycles of internal pressure and axial straining is simulated in ANSYS for the same geometry and results are compared with those obtained by experimentation in section of this paper.

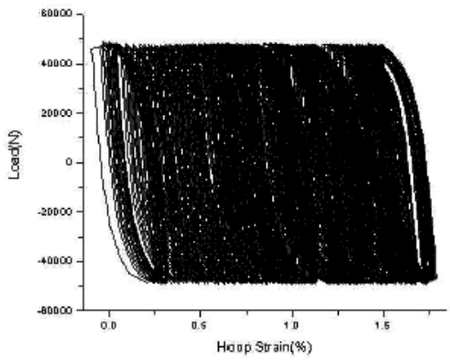

Figure 12- Plot of Axial Load vs. Hoop Strain for Biaxial Ratcheting Test

7. CHABOCHE MATERIAL MODEL

The main reason for kinematic hardening is the dislocation pile up. In plastic deformation, dynamic recovery takes place which lowers the dislocation density and thus effective rate of strain hardening is reduced. The linear kinematic hardening and multilinear models produce closed Hysteresis loop and hence, cannot simulate a uniaxial ratcheting response also.When slight nonlinearity is introduced into the Multilinear Ohno-Wang model, it shows promise in simulating both uniaxial and biaxial ratcheting responses. The most well known nonlinear kinematic hardening rule was proposed by Armstrong and Frederick (1966). They introduced a kinematic hardening rule containing a 'recall' term essentially makes the rule nonlinear in nature

$$da = \frac{2}{} c d\varepsilon^{p} - \gamma a dp, \qquad (1)$$

where

$$dp = \left| d\varepsilon^{p} \right| = \left[\frac{2}{3} d\varepsilon^{p} \bullet d\varepsilon^{p} \right]^{1/2} \qquad (2)$$

The recall terms brings decay in the back stress vector to take into account dynamic recovery. For uniaxial stress cycle with mean stress, the recall term g produces change in shapes between forward and reverse loading paths. Therefore the loop does not close and results in ratcheting. For continued cycles between two fixed stress levels, this model simulates the same ratcheting loops for all the cycles and thus, produces a constant ratcheting rate (strain accumulation per cycle). In actual experimentation, it is observed that the loading curves gradually stiffen while the unloading curves soften with cycles. This results in the gradual decrease in the rate of ratcheting and subsequent stabilization to a constant rate of ratcheting. Conceptually, the Armstrong-Frederick model has been a leap in representing cyclic plasticity responses of the materials, but is not robust enough to predict the ratcheting responses of the materials. It was later observed by Chaboche that recovery mechanism is not working on same manner for small and large strains. So he proposed the decomposition of back stress into short and long range. Short-range back stress corresponds to internal stress variations associated with non-uniform dislocation distribution and saturates quickly. The long-range back stresses are stress fluctuations across the heterogeneous substructures. They are slow to change over large strain amplitudes. MacDowell and Chaboche proposed additive decomposition of the back stress term. Thus the Chaboche kinematic hardening rule is a superposition of several Armstrong-Frederick hardening rules. Each of these decomposed rules has its specific purpose.

$$da = \sum_{i=1}^{M} da_i, da_i = \frac{2}{3} c_i d\varepsilon^{p} - \gamma_i a_i dp \qquad (3)$$

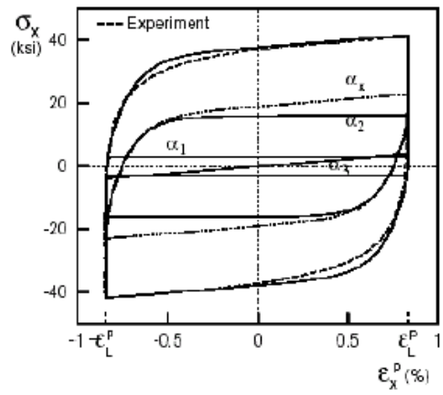

Figure 13- Comparison of the Stable Hysteresis Loop obtained with Experimentation and the Chaboche Model (Reproduced from a Paper by Choboche)

A stable hysteresis loop (Figure. 13) can be divided into three segments where Armstrong-Frederick model fails: the initial high modulus at the onset of yielding, the constant modulus segment at the higher strain range and the transient nonlinear segment (Knee of the hysteresis loop). They suggested that first rule (α_1) should start hardening with very large modulus and stabilize very quickly. The second rule (α_2) should simulate the transient nonlinear portion of the stable hysteresis curve. Finally the third rule (α_3) should be a linear hardening rule (γ_3=0) to represent the subsequent linear part of the hysteresis curve at high strain range. The Chaboche model is the robust model developed so far using the yield surface theory and the Armstrong-Frederick Kinematic hardening rule and the work presented in this project is concentrated on this model. Here, the detailed parameter determination scheme for this model is explained and parameters are drawn for SS 304 material and tuned for uniaxial ratcheting responses.

7.1 Evolution of the Chaboche Model

We need variation of backstress (α_x) with respect to plastic strain (ε_p). For uniaxial loading, this αx is same as that of 'a' which is centre of yield surface in deviatoric stress space. α_x is decomposed into three hardening rules as discussed earlier.

$$\alpha_x = \sum_{i=1}^{3} \alpha_i \tag{4}$$

Also for the loading part of the Hysteresis loop,

$$\sum_{i=1}^{3} \alpha_i + \sigma_0 = \sigma_x \tag{5}$$

All parameters, except γ_3, are determined from a uniaxial stable hysteresis loop. This required a hysteresis loop of reasonable strain limit as shown in Figure. 4 which ensures that all, except the third slightly nonlinear kinematic hardening variable get stabilized within the strain limit. Figure. 14 shows the variation of axial stress and backstress (α_x) with respect to axial plastic strain. This variation is obtained from the stable hysteresis loop. (Figure. 4)

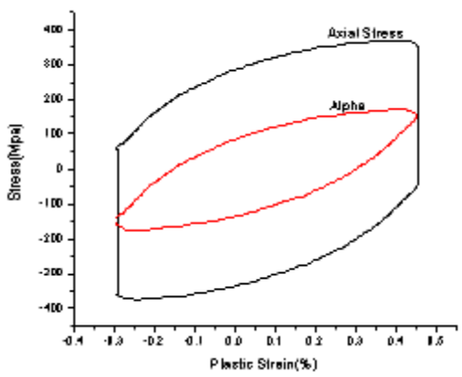

Figure 14 - Plot of Axial Stress and Back stress vs. Plastic Strain Obtained from Experimentation

7.2 Mathematical Formulation of the Chaboche Model

For uniaxial loading case, we have

$$F = |\sigma - \alpha| - \sigma_y = 0 \tag{6}$$

$$d\varepsilon^p = \frac{1}{E^p} d\sigma \tag{7}$$

$$d\alpha = c\,d\varepsilon^p - \gamma\alpha\,|d\varepsilon^p| \tag{8}$$

$$E^p = c \mp \gamma\alpha + \frac{d\sigma_y}{d\varepsilon^p} \tag{9}$$

Where – and + correspond to loading and reverse loading respectively. E^p is the plastic modulus for the loop (H).

During tensile or positive loading, it follows that

$$d\sigma = (c - \gamma\alpha)\,d\varepsilon^p \quad (10) \quad \text{and} \quad E_t^p = c - \gamma\alpha + \frac{d\sigma_y}{d\varepsilon^p} \quad (11)$$

When the loading direction is reversed, the plastic flow is compressive:

$$d\sigma = (c + \gamma\alpha)\,d\varepsilon^p \text{ and } E_c^p = c + \gamma\alpha + \frac{d\sigma_y}{d\varepsilon^p} \tag{12}$$

where the subscripts t and c stand for tensile and compressive loading, respectively. These equations are explained schematically in Figure. 15.

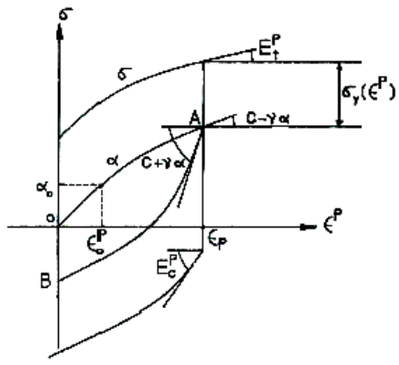

Figure 15 - Illustration of Hardening Modulus for Loading and Reverse Loading

As is clear from the figure, the effects introduced by the recall term on the tensile and compressive plastic flow are different. Assuming that $\gamma > 0$, the hardening modulus for reverse plastic flow is higher than for original loading at a given plastic strain ε^P Therefore the relation between α and ε^P is nonunique, and the nonlinearity and the concavity of the stress-strain curve is correctly produced. One of the merits of the nonlinear kinematic hardening model is that for uniaxial loading, it can be integrated to obtain the analytical solution. Indeed, beginning with any $\varepsilon^P{}_o$ and α_0 as shown in Figure 15, for c and γ constant, we can integrate the above equation to get

$$\alpha(\varepsilon^p) = \frac{c}{\gamma} + \left(\alpha_0 - \frac{c}{\gamma}\right)\exp\left\{-\gamma\left(\varepsilon^p - \varepsilon_0^p\right)\right\} \tag{13}$$

Where α (ε^p) and ε^p represent any point on the half cyle OA. Similarly for the another half cycle AB, We obtain the following

$$\alpha(\varepsilon^p) = -\frac{c}{\gamma} + \left(\alpha_0 + \frac{c}{\gamma}\right)\exp\left\{\gamma\left(\varepsilon^p - \varepsilon_0^p\right)\right\} \tag{14}$$

We can combine these two equations as

$$\alpha(\varepsilon^p) = \pm\frac{c}{\gamma} + \left(\alpha_0 \mp \frac{c}{\gamma}\right)\exp\left\{\mp\gamma\left(\varepsilon^p - \varepsilon_0^p\right)\right\} \quad (15)$$

where the sign on the top corresponds to tensile plastic flow and that below to the compressive flow. we can now write the stress-strain curve for uniaxial cases:

$$\sigma = \alpha(\varepsilon^p) \pm \sigma_y(\varepsilon^p)$$
$$= \pm\frac{c}{\gamma} + \left(\alpha_0 \mp \frac{c}{\gamma}\right)\exp\left\{\mp\gamma\left(\varepsilon^p - \varepsilon_0^p\right)\right\} \pm \sigma_y(\varepsilon^p) \quad (16)$$

For pure kinematic hardening model, the isotropic hardening is not present during the cyclic loading.

$$\frac{d\sigma_y}{d\varepsilon^p} = 0 \quad (17)$$

7.3 Parameter Determination Scheme

We have two nonlinear and one linear hardening rule for Chaboche's model. For, first two rules, plastic modulus becomes zero within the strain range of hysteresis loop. So the backstress terms $\alpha 1$ and $\alpha 2$ becomes stabilized at high strain range to c/γ. A stabilized 'decomposed' backstress ($\alpha 1$ and $\alpha 2$) should have the same tensile and compressive levels within the strain range of the stable loop. In other words, for the loading portion of the hardening curves (α vs . ε^p), they should start from $-c_i/\gamma_i$ at the starting plastic strain - $\varepsilon^p{}_L$ and reach the value c_i/γ_i at or prior to the final plastic strain - $\varepsilon^p{}_L$. In addition, the third linear backstress α_3 should pass through the origin.

Putting $\alpha_0 = -c_i/\gamma_i$ and $\varepsilon_0^p = -\varepsilon_L^p$ we get

$$\alpha_i = \frac{c_i}{\gamma_i}\left[1 - 2\exp\left\{-\gamma_i(\varepsilon_x^p - (-\varepsilon_L^p))\right\}\right], \quad (18)$$

for i=1 and 2

and $\alpha_3 = c_3\varepsilon_x^p$

c_1 should be a very large value to match the plastic modulus at the yielding and corresponding γ_1 also should be large enough to stabilize the hardening of α_1 immediately. c_3 is determined from the slope of the linear segment of the Hysteresis loop at a high strain range. c_2 a n d γ_2 are evaluated by trials to produce a good representation of the experimental stable Hysteresis curve which should also satisfy the relationship

$$\frac{c_1}{\gamma_1} + \frac{c_2}{\gamma_2} + \sigma_0 = \sigma_s - \frac{c_3}{2}\left\{\varepsilon_x^p - (-\varepsilon_L^p)\right\} \quad (19)$$

7.3.1 Actual Parameters Obtained

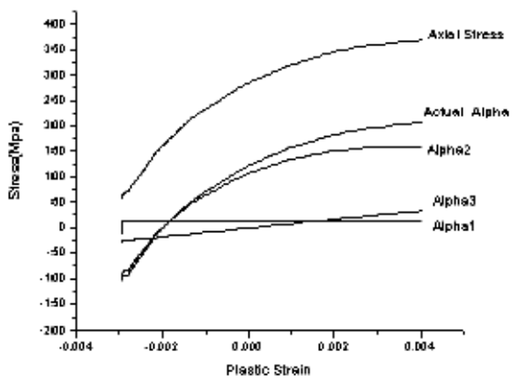

Figure 16- Variation of Decomposed Backstresses against Plastic Strain

c_1 is taken as 3x105 Mpa and γ_1 of 20000 such that α_1 stabilizes immediately starting from -15 and stabilizing to 15 Mpa. The value of c_3 was found to be 8584.13 Mpa. So we get α_1 and α_3. α_2 is obtained by subtracting α_1 and α_3 from α_x value obtained experimentally in Fig. 14. After this, the task remained is to find the value of c_2 and γ_2 such that the calculated α_2 from Equation matches with the α_2 obtained with subtraction of α_1 and α_3 from α_x. This is done by trial and error and the values decided to give the good fit are c_2 = 7.5 x10^4 Mpa and γ_2 = 530. The value of γ_3 will be chosen from the uniaxial ratcheting test.

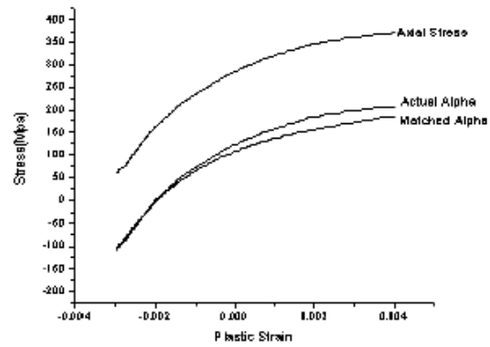

Figure 7- Plot of Actual and Matched Backstress vs. Plastic Strain

The variation of decomposed backstress against the plastic strain is shown in Figure 16 for the loading part of the curve. Here variation of actual stress and backstress is also shown to get the feel of these decomposed values. The total value of calculated backstress and the exact one obtained from the

experimentation are shown against the plastic strain in Figure - 17. Here it can be seen that the both matches almost exactly.

7.3.2 Tuning for γ_3 Value

The tuning of the γ_3 value is done with preparing a finite element model of the pipe in ANSYS and subjecting the same against the uniaxial stress controlled loading of mean stress 75 Mpa and Stress Ratio -0.6. This loading is same as that of the uniaxial ratcheting test conducted on the tube. A tube model is prepared in ANSYS with SHELL181 elements. The one end is restricted against all degrees of freedom and at the other end, stress controlled load cycles are applied. The initial value of γ_3 for the Chaboche model is assigned as zero for the first simulation. Figure 18 shows the plot of tube modeled with this element in ANSYS.

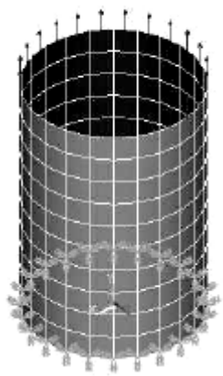

Figure 18- Tube Model with SHELL181 for Ratcheting Simulation

The model is first checked for its accuracy for loads in elastic loading. It was confirmed that the stress states are uniform in the entire model for applied axial loads as desired. Then the model is subjected to the same loading history as mentioned above for 100 cycles. Here the value of γ_3 is kept initially as zero. It was found that the model gives shakedown immediately in first few cycles. So value of γ_3 was increased slowly in terms of 0.25 and it was found that at value of 0.75, experimental and FEM results match exactly for 100 cycles of test. The trend of ratcheting was almost linear and there was no indication of any shakedown as observed in the experiment. Figure19 shows the plot of axial stress vs. axial strain for the 100 cycles of the test in ANSYS. Figure 20 shows the plot of axial strain vs. the number of cycles for 100 cycles applied. Use of this material model of SS 304 will be made for further ANSYS simulations in the next section and will be compared with experimental results.

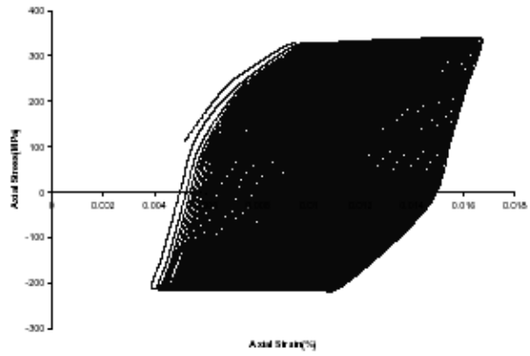

Figure 19- Plot of Axial Stress vs. Axial Strain for 100 Cycle Simulation

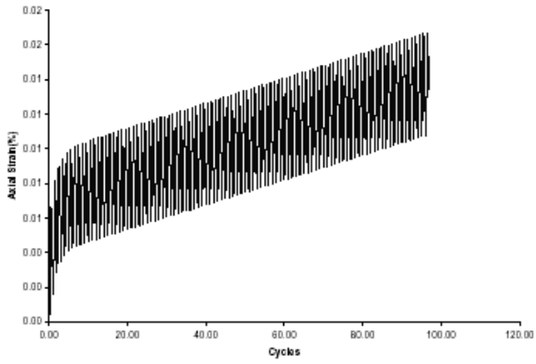

Figure 20- Plot of Axial Strain vs. Number of Cycles

8. SIMULATIONS CARRIED OUT IN ANSYS

The next task after finding out the material parameters is to carry out thesimulations for different geometries and load histories using the finite element method (FEM). These results can be compared with those obtained by experimentation and some useful conclusions can be drawn from this comparison. Finally, this material model can be used to simulate ratcheting behavior for real complex geometries and load histories. In order to model the ratcheting behavior at both material and structural level, a general purpose finite element program is needed. The program should have non-linear, plasticity and large deflection/deformation capabilities; open architecture (for possible customized version by user); and be readily available. ANSYS meets all the requirements and thus has been used in this work there are three ingredients in the rate independent plasticity theory in the ANSYS program: the yield criteria, flow rule and the hardening rule. An Euler backward scheme is used to enforce the consistency condition. This ensures that the updated stress, strains and internal variables are on

the yield surface. Here the Euler backward integration scheme is the radial return algorithm for the von Mises criteria. If the stress exceeds the material yield, the plastic multiplier to be used in the flow rule is determined by a local Newton- Raphson iteration procedure. The detailed algorithm is available in the ANSYS Theory Manual.

8.1 Simulations for Tests Done at Experimentation

The Tube FE model was subjected to second uniaxial load history of the experimentation done (mean stress of 278 Mpa and stress ratio 0.54) as discussed earlier. It was found that the ANSYS produces same amount of accumulation as that obtained by experimentation. This means that the current Chaboche material model is tuned correctly for the uniaxial ratcheting tests.

So one can say that this material model of SS 304 will give exact results for uniaxial tests of any loading history and on any geometry. As we have data for the biaxial test conducted on tube specimen, the same model was subjected to loading history of internal pressure and axial strain cycling. The exact number of cycles for axial strain cycling with 100, 200 and 250 bar internal pressure were counted from the experimental data and the macro was prepared for the same in ANSYS. The axial strain cycling was for ±0.5%.

The model was subjected to biaxial loading history of about 389 cycles. The Figure 21 shows the plot of accumulated hoop strain against the axial strain. The Figure 22 shows the plot of hoop strain accumulation against applied axial strain cycles. In both these plots, we can clearly identify the three regions of constant primary load of 100 bar, 150 bar and 200 bar. The test with 100 bar has reached shakedown at hoop strain of 0.32% (refer Figure 11). Here using ANSYS, the shakedown was obtained at 0.75% hoop strain accumulation. So ANSYS over predicted the results as compared to actual results. Also total strain accumulation after 389 cycles given by ANSYS is 4% which is much higher than the strain accumulation at shakedown for actual test sample (1.8%)

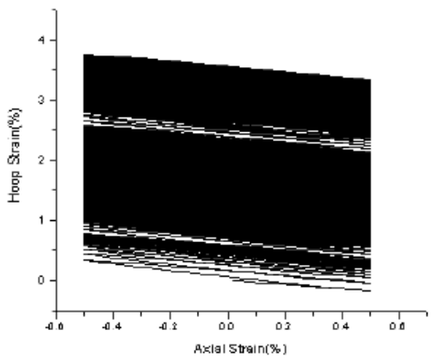

Figure 21- Plot of Hoop Strain vs. Axial Strain for Biaxial Simulation

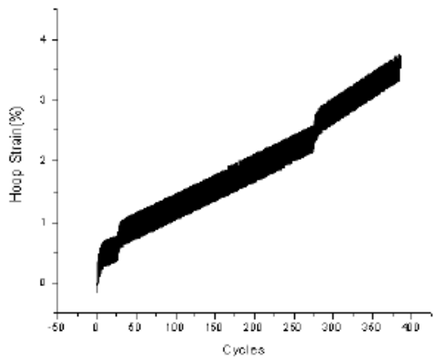

Figure 22- Plot of Hoop Strain vs. Axial Strain Cycles for Biaxial Simulation

8.2 Reason for the Overprediction by ANSYS

As we have seen that the Chaboche model shows promise to simulate the uniaxial behavior but overpredict ratcheting for biaxial behavior. Such performance by the models is related to an inherent feature of modeling—simulations of ratcheting responses in uniaxial loading primarily depend on the plastic modulus, whereas the simulations in multiaxial loading depend on both the plastic modulus and the kinematic hardening rule, with significant influence from the latter. This feature is elaborated through Figure-23 .

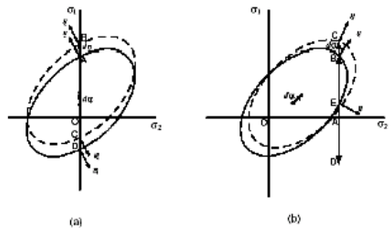

Figure 23 -Yield Surface Translation and Normal Directions during a) Uniaxial Loading and b) Biaxial Loading Cycles

For a uniaxial load increment AB, in Fig. 23 a), the normal direction, $\underset{\sim}{n}$ at the stress point B remains parallel to that at A irrespective of the kinematic hardening rule adopted in a model. This is also true for an increment CD during reverse loading. As a result, during uniaxial loading cycles OBDBD., direction and magnitude of the term $\partial F/\partial\sigma$ in the flow rule remain unchanged and the plastic strain increments become a function of the plastic modulus (H) only. Therefore, simulations of uniaxial ratcheting responses depend entirely on the accuracy of the plastic modulus calculation of a model. This feature in multiaxial

loading is demonstrated for a biaxial loading history OACDCD....., obtained by superimposing a constant σ2 stress to a stress cycle along σ1 (Figure. 23 b), which is a small deviation from the uniaxial loading cycle in Figure.23(a). During a biaxial loading increment BC (Figure. 23 b), normal direction at C changes from that at B. Similar changes occur continuously throughout the loading history. It is clearly observed in Figure. 23 that normal directions in biaxial loading are significantly different from those in uniaxial loading. This change in normal direction during the biaxial loading results from the shift of the stress point along the yield surface when it translates. Hence, the normal direction in multiaxial loading is a function of the direction and magnitude of the yield surface translation, which, in turn, is dictated by the kinematic hardening rule of the model. Different kinematic hardening rule produces different translation direction and, thereby, greatly varied normal directions for a given stress history. As a result, the simulation of ratcheting responses under multiaxial loading by a plasticity model depends significantly on its kinematic hardening rule. In present algorithm used by ANSYS incorporating the Chaboche model, the plastic modulus (*H)* is calculated using the kinematic hardening rule and the consistency condition. The parameters of the kinematic hardening rules are determined from uniaxial loading responses. These parameters are, in effect, calibrated to produce a better representation of the plastic modulus only, and consequently, fall short in predicting the representative yield d surface translation and subsequent normal directions.

9. CONCLUSIONS

The parameters of Chaboche model obtained here show correct simulation of the hysteresis loop and also uniaxial ratcheting. The reason for this is due to the fact that the plastic modulus calculation is much improved in this model as compared to multilinear or Armstrong-Frederick model. Simulations of uniaxial ratcheting responses depend entirely on the accuracy of the plastic modulus calculation of a model. So Chaboche model is robust enough for simulating hysteresis loop and the uniaxial load responses. For the biaxial case, the general trend of hoop strain accumulation was same for both experimental and FEM results. The FEM overpredict results than the actual obtained by experimentation. The reason for this is due to inability of the Chaboche model in predicting the representative yield surface translation and subsequent normal directions. The simplified assumption of keeping the shape of yield surface constant during the hardening rule for simulation of phenomena where considerable distortion takes place might have lead to this overprediction. Then there is need to include the change in shape of yield surface during the plastic loading.

10. REFERENCES

1. Ponter A.R.S., Cocks A.C.F.,1985,*"The Plastic Behavior of Components subjected to Constant Primary Stresses and Cyclic Secondary Strains"*, Journal of Strain Analysis, Vol. 20, pp.7-14.
2. Hassan T., Corona E. and Kyriakides S., 1996*, "On the Performance of Kinematic Hardening Rules in Predicting a Class of Biaxial Ratcheting Histories",* International Journal of Plasticity, Vol. 12, No. 1, pp. 117-154.
3. Ohno N., Abdel-Karim M., Mima Y., Mizuno M., 2000 *"Uniaxial Ratcheting of 316FR Steel at Room Temperature-Part I: Experiments",* ASME Journal of Engineering Material and Technology, Vol.122, pp.29- 34.
4. Hassan T. and Kyriakides S., 1994, *"Ratcheting in Cyclically Hardening and Softening Materials; Part I Uniaxial Behavior"*, International Journal of Plasticity, Vol.10, pp.149-184.
5. Hassan T. and Zhu Y. and Matzen V.C., 1998, *"Improved Ratcheting Analysis of piping components",* International Journal of Pressure Vessels and Piping, Vol.75, pp.643-652.
6. Hubel H., 1996, *"Basic Conditions for Material and Structural Ratcheting",* Nuclear Engineering and Design, Vol.162, pp. 55-65.
7. Ohno N. and Wang J.D., *1993 "Kinematic Hardening Rule with Critical State of Dynamic Recovery, Part I: Formulations and Basic Features for Ratcheting behavior",* International Journal of Plasticity, Vol. 9, pp.375-390.
8. Khan A.S. and Huang S., 2000, *"Continuum Theory of Plasticity",* John Wiley and Sons Inc New York,
9. Hassan T. and Bari S., 1995, *"Anatomy of Coupled Constitutive Models for Ratcheting Simulation",* International Journal of Plasticity, Vol. 16, pp. 381-409.
10. Chaboche J.L., and Nouailhas, D.,1988 *"Constitutive Modeling of Ratcheting Effects—Part I: Experimental Facts and Properties of the Classical Models",* ASME Journal of Engineering Materials and Technology, Vol.111, No. 4, pp. 384–392.
11. Hassan T. and Bari S., 2002, *"An advancement in cyclic plasticity modeling for multiaxial ratcheting simulation",* International Journal of Plasticity, Vol. 18, pp. 873-894.
12. Ohno N. and Wang J.D., 1993, *"Kinematic Hardening Rule with Critical State of Dynamic Recovery, Part II: Applications to Experiments of Ratcheting Behavior",* International Journal of Plasticity, Vol. 9, pp.375-390.